CHAPTER–V

Modelling of Potato Late Blight Disease Severity using Field Based Hyperspectral Observation

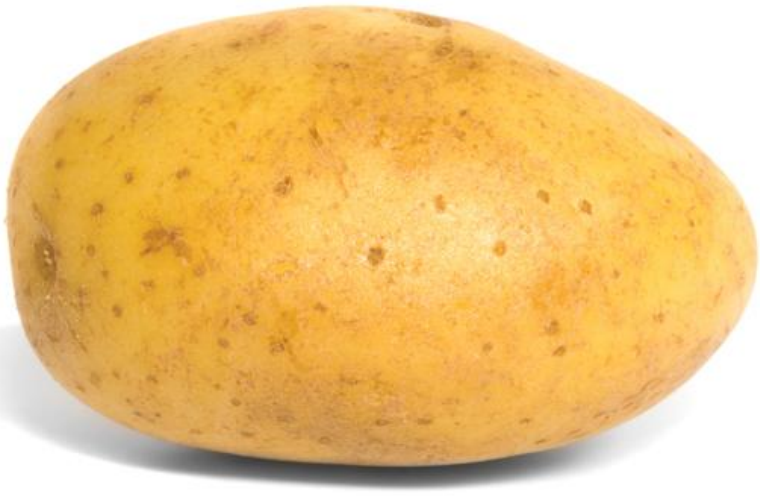

MODELLING OF POTATO LATE BLIGHT DISEASE SEVERITY USING FIELD BASED HYPERSPECTRAL OBSERVATION

5.1 Introduction

Pest and diseases can significantly reduce the economic yield of crops and make the condition vulnerable to the resource poor farming communities. Advance prediction of disease congenial weather over short and medium temporal scale and adopting appropriate and judicial protection strategy can substantially contribute towards food security. Understanding the disease cycle and optimum weather conditions towards infestation and dissemination can improve our ability to monitor the disease epidemic and take preventative measures to avoid economic loss and environmental degradation by using overdose of pesticides.

The science of disease occurrence and its dispersal mechanism is well known but how to take proactive preventive measures over large crop growing area has always remained a major challenge especially under dynamic weather condition. In case of potato late blight (*Phytophthora infestans*) disease under warm temperature and prolonged periods of leaf wetness, sporangiophores emerge from the stomata and release numerous airborne sporangia causing a rapid dispersal of the disease and the infection becomes apparent in 3 days. Keeping in view the temporal constraints and large spatial extent the manual method of diagnosis and scheduling pesticide application in near real time is impractical. In contrast Remote Sensors provide a synoptic view of the crop growing area at a time and the anomalies in crop vegetative growth can be picked up at different temporal scale using satellite data processing techniques. The disease causes change in the chlorophyll content and plant biophysical parameters which are discernible in the red and near-infrared region of the electromagnetic spectrum. By careful selection of multi-spectral remote sensing and weather satellite data integrated with limited ground intelligence it is possible to forecast the disease congenial condition under different crop regime. In comparison to the multi-spectral and super-spectral data the sampling frequency of the hyperspectral data is much high to the tune of 5-10 nm which is good enough to capture the subtle spectra features caused by vegetation anomaly. Hyperspectral sensors have advantage over multi-spectral image by virtue of large number of narrow and contiguous spectral wave bands extending from visible to near-infrared region (350-2500 nm).

Typically green leaves show absorption at blue and red region of the spectrum caused by plant pigments whereas sharp increase is apparent in the infra-red region caused by high scattering at the interfaces of the mesophyll cells (Gausman, 1974 and 1977; Slaton et al., 2001). This contrasting spectral behaviour forms the basis for monitoring and managing crop and natural vegetation communities (Knipling, 1970; Bauer, 1975). Due to biotic / abiotic stress and / or senescence chlorophyll concentration decreases. These results in flattening of the red absorption well decrease in the IR reflectance and overall increase in the reflectance. Besides the reflectance the location of the red-edge (i.e. the maximum slope between red absorption and IR reflectance) shifts towards shorter wavelength with stress which serves a proximal indicator of stress.

Two of the major hydroxyl absorption band in the NIR region is centred around 1450 and 1950 nm which are influenced by the water content in the plant tissues. The absorption bands are very deep and sharp in case of healthy green plants at full vegetative growth stage and the depth decreases with water stress / plant senescence. However, the spectral signature of standing vegetation in the field is much more complex due to mixture of discrete plant parts, soil background, shadow etc. Moreover the reflectance at canopy level and leaves are also different.

Hand held Spectro-radiometer data in conjunction with airborne and spaceborne hyperspectral data are being widely used for detecting plant stress (Carter, 1988), crop moisture variation (Pen˜uelas et al. 1995) as well as disease detection and monitoring (Huang et al., 2007). The studies of Malthus and Madeira (1993) showed the changes of spectral spectral reflectance properties in visible and NIR region due to infection of Botrytis disease in faba bean. Spectral characteristics of rice plants affected by brown plant hopper (*Nilaparvatalugens)* at different severity level was investigated by Yang and Cheng (2001) who have shown significant differences in reflectance at wavelengths of 755 and 890 nm. Bravo et al. (2003) have classified of yellow rust infected wheat plants and healthy plants by using hyperspectral and quadratic discriminating model. Zhang et al. (2003) developed a MNF approach to discriminate the late blight (*P. infestans*) disease affected tomato plant from the healthy one by using hand-held spectrometer data. The classification results successfully separated the diseased tomato plants at 3 severity level.

Generally for plant disease identification band combination methods have widely been used (Larsolle et al., 2007). The sensitivity of waveband to detect plant disease depends on how the disease interacts with a specific crop species (Mahlein et al., 2013). From most of the previous

studies it was found that the most sensitive bands are commonly located in the visible and NIR region for crop disease detection (Cheng et al., 2010). Spectral vegetation indices derived from VNIR region of spectrum are widely used for crop health monitoring, including biochemical and bio-physical parameters. Apan et al. (2004) used discriminant analysis to determine which narrow band indices were the best indicators of plant stress caused by the orange rust disease in sugarcane using Hyperion image. They found that indices developed using red edge spectra were poor indicators of disease. Indices using only NIR wavelengths performed moderately better. The best indices were those using the 1600 nm short wave infrared band in a ratio with either an 800 nm NIR band or 550 nm green band.For estimating real-time applications of fungal disease severity Muhammed (2005) used hyperspectral crop reflectance data of wheat and established a procedure to detect the disease severity level with low computational load. The studies of several hyperspectral indices were carried out by Genc et al. (2008) to detect the sunn-pest (Eurygaster integriceps) of wheat and it was found that for assessing their damage levels NDVI and SIPI were more suitable. Ray et al. (2011) investigated the sensitive narrow bands by using hyperspectral indices to differentiate healthy and PLB disease affected potato crops. By using the spectral derivative method it was able to differentiate the disease affected potato crop spectra according to the PLB disease severity. Jones et al. (2010) studied reflectance spectroscopy of ultraviolet, visible and NIR to quantify the disease severity of *Xanthomonasperforans* affected tomato leaves and found that the wavelength region of 750–760 nm was highly sensitive to the disease. The sensitive bands specific to the brown spot fungal disease of rice was investigated by Liu et al. (2008) using hyperspectral data. The disease detection possibilities using spectral reflectance data was reviewed by Sindhuja et al. (2010). Besides, several vegetation indices were established to quantify the plant diseases (Huang et al., 2007; Mahlein et al., 2013; Feng et al., 2016). To detect spectral changes and disease development, multivariate analysis tools like neural networks (Castro et al., 2012), PLSR method (Zhang et al., 2012a, b, 2014), factor analysis and back propagation neural network (Shen et al., 2015b) was also applied.

When the potato plant is affected by pathogen, the enzyme activity of leaf and cell energy metabolism function is affected as well as the internal structure of leaves are changed. As a result the spectral reflectance increases in visible and SWIR region due to the changes of chlorophyll content and decreases in NIR reflectance due to lack of water content. These typical characteristics of spectral reflectance differentiate the disease affected potato crops from the healthy one (Cheng et al., 2010; Zhang et al., 2012a). To evaluate the changes of chlorophyll density of disease affected wheat canopy Feng et al. (2013) investigated the Normalized

Difference Angle Index (NDAI) and found reliable results. From the above finding it is suggested that the hyperspectral remote sensing technology have unique feasibilities to detect the crop disease as well as to rapid and convenient evaluation of physico-chemical response to crop disease.

In the present study field spectra was collected from various potato growing fields of the Hooghly and Paschim Medinipur districts wherein the canopy and leaf spectra of both the healthy and diseased plants were collected at different stages of disease intensity using HR 1024 Field Spectro-radiometer. Several spectral derivatives and vegetation indices sensitive to plant stress were constructed to establish correlation with disease severity and spectral variables.

5.2 Objectives

The main objectives of the present study are in the following,

- To study of spectral characteristics of healthy and late blight affected potato canopy and changes in spectral pattern with disease severity.
- To establish a relationship between hyperspectral indices and potato late blight disease severity for remote monitoring.

5.3 Material and Methodology

5.3.1 Locations of Field Based Hyperspectral Data Collection

The field based hyperspectral observation was taken at various locations of the Hooghly and Paschim Medinipur district of West Bengal (Fig. 5.1). The observations were collected during 2013 and 2014 synchronized with field reporting on initiation and advanced stages of disease. The dates of field visits were 2nd, 3rd and 21st February of 2013 in case of Hooghly and 21st January, 25th January, 5th February and 9th February of 2014 for Paschim Medinipur district respectively during which the disease becomes epidemic. In this region the major

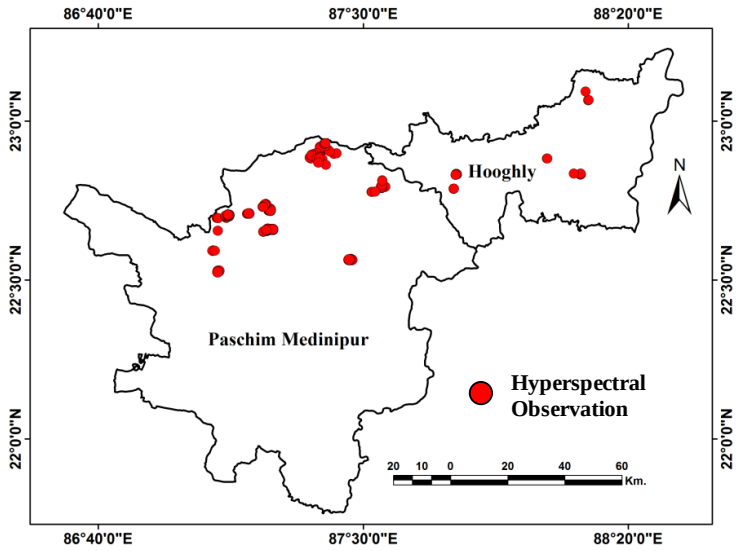

Figure 5.1: Locations of Hyperspectral Observation

variety of potato is Kufri Jyoti sown in line with row to row spacing of 20 cm and plant to plant of 18 cm. The date of sowing varied between 1^{st} and 2^{nd} week of November. But sometimes based on the prevailing weather condition of Paschim Medinipur, the time of sowing is extended up to the 3^{rd} week of November.

5.3.2 Field Hyperspectral Measurements

Hyperspectral observations of potato leaves and canopy were collected from a distance of 2.5 m vertically above the canopy, using a portable Field Spectroradiometer (HR-1024) during 2^{nd} week of January to 2^{nd} week of February in Hooghly and Paschim Medinipur district during which the PLB disease is most prevalent. Potato plants at various degrees of infection severities were selected for field spectra collection. To apportion the effect of soil background, the spectra of bare soil was also collected from the field. The instrument records spectral reflectance between 350-2500 nm with sampling interval of 1.4 nm (FWHM = 3 nm) for 350 – 1000 nm and 2 nm (FWHM=10 NM) for 1000-2500 nm spectral region. Radiometer was equipped with a 14^0 field-of-view lens and was positioned by pointing downward to measure the upwelling radiance from the potato canopy. The height above the top of the canopy of the radiometer was kept constant (2.5 m) throughout the observation, yielding a sampling area with a diameter of 61 cm on the ground corresponding to an area of 2920 cm^2. The centre of the instrument's FOV was marked using laser pointer of HR-1024 instrument. A tape measuring 61 cm length was placed horizontally above the canopy, the centre of which is coincident with the centre of instrument's FOV (Figure 5.2). The objective was to capture the vertical photograph of each observation point that represents the footprint of the Spectroradiometer lens. The radius of the instrument's footprint at nadir looking viewing geometry was calculated as follow:

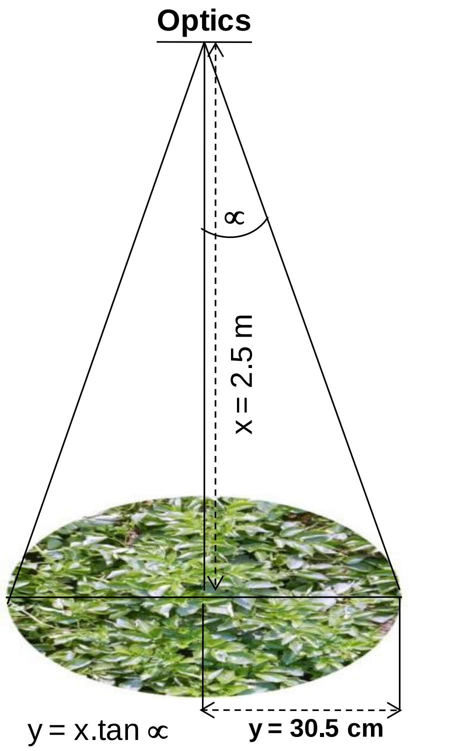

Figure 5.2: Observation Geometry

$$y = x * \tan(\alpha) \quad \ldots\ldots\ldots\ldots \quad (1)$$

Where

y = radius of ground footprint

x = perpendicular distance between optics and top of the object

α = Field of view (full angle) / 2

Radiometer was configured to take 15 simultaneous upwelling irradiance measurements, which were internally averaged and stored as a single data file. The measurements were performed during solar noon (i.e. solar angles between 12:00 and 14:00 IST) when the solar zenith is minimal. A white Spectralon reflectance standard was used to calibrate the Spectrometer to the total incoming radiant flux. The spectrometer was re-calibrated after every 4^{th} observation in each plot. All the canopy radiance data were normalized and converted into bi-directional reflectance factor (%) using measured radiance of calibration panel per wavelength. Raw data of HR-1024 was corrected for signature file overlap/matching. After the removal of outliers, the data was smoothened following least square 2^{nd} order polynomial fit technique (Savitzky-Golay, 1964) which helped to suppress the noise and at the same time retained the shape of the original signal. Although noise was not apparent in the visible range, but a considerable amount of noise was minimized in 915 to 1000 nm region.

5.3.3 Signature File Overlap/Matching

Once the data is downloaded from the HR-1024 PDA, it was corrected for signature file overlap / matching. Spectrum averaging is performed in post-processing environment using SVC HR-1024 PC Data Acquisition software. It is especially useful when signal strength is very low in the outdoors at around 1400 and 1900 nm, due to the absorption by water vapour in the atmosphere. When checked, the Silicon and SWIR1 data are combined (within the overlap region) using a combination of the two overlapping detector data sets. Using this option only affects the data within the Overlap region. In the present study in 'matching type' "Reflectance" option is selected which combines the reference and target scans into a reflectance curve, and uses this curve's data to perform matching.

5.3.4 Noise Removal and Data Smoothening

The detector overlap corrected data was checked for valid values. After removal of outliers the data was smoothen following Savitzky-Golay (1964) least square polynomial fit technique which helps to minimize the noise and at the same time retains the shape of the original signal.

5.3.5 Data Normalization

To compare data across various dates of observation it is necessary to normalize the data with respect to population mean and standard deviation. Normalization process corrects the illumination variation and makes data comparable across different dates of observation. All the data sets were normalized using formula,

$$R_{norm} = (R_{ori} – R_{mean}) / R_{sd} \quad \ldots\ldots (2)$$

Where

R_{norm} = Normalized value of spectral reflectance

R_{ori} = Spectral reflectance value of original data

R_{mean} = Mean spectral reflectance value of original data

R_{sd} = Standard deviation of the original spectral reflectance data

5.3.6 Continuum Removal and Characterization of Spectral Absorption Features

Each spectra is composed of an albedo and a absorption component. The albedo component gives the overall shape of the spectral curve whereas the absorption features are characteristics of electronic processes in the given electromagnetic spectrum. The prerequisite for absorption feature analysis is to remove the continuum (Clark and Roush, 1984) of the spectra which is used to place all of the absorption features on a common reference plane. The continuum was calculated using 2nd order polynomial fitted to selected channels (channels without absorption features) in the relative reflectance spectra. The continuum was then removed by dividing the polynomial function into the actual data. Mathematically it is carried out by dividing the reflectance value 'R' for each point in the absorption pit by the reflectance level of the continuum line (convex hull) R_c at the corresponding wavelength. The values of the output curves vary between 0 and 1(Fig. 5.2), in which the absorption pits are enhanced and the absolute variance is removed (Schmidt and Skidmore 2003). Once the continuum is removed, the absorption feature can be characterized in terms of its band depth, full width at half maximum, band centre and asymmetry, which is used in spectral feature fitting algorithm also.

In the visible region continuum removal was applied on two major spectral regions e.g. 450-550 nm and 550-750 nm, which are characteristics to chlorophyll absorption and is relatively noise free. Although 550–750nm is strongly influenced by pigment absorption, several studies have

established relationships between reflectance at specific wavelengths in this region and other foliar bio-chemicals (Ponzoni and Goncalves 1999, Curran et al. 2001, Gong 2002), largely emanating from the interrelationships between foliar bio-chemicals themselves.

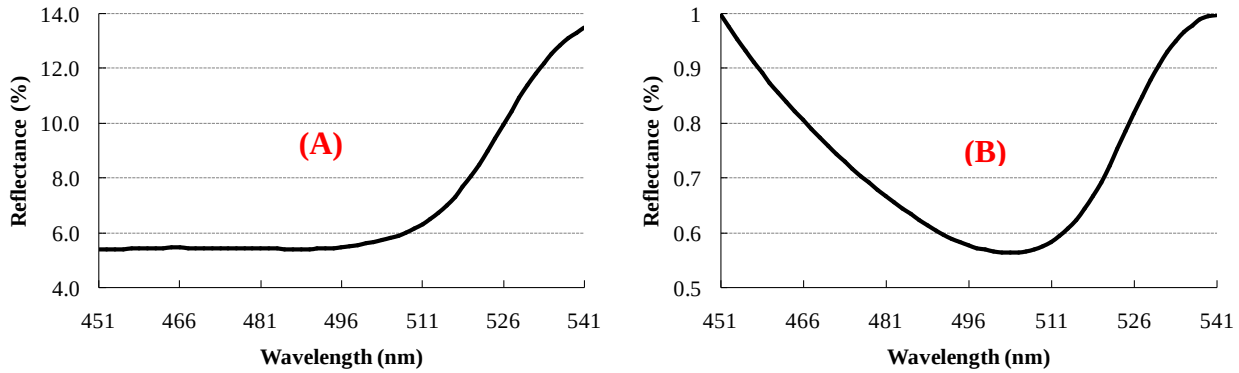

Figure 5.3: (A) shows the Spectra with Continuum in 450-540 nm and Figure (B) Shows the Continuum Removed Spectra in 450-540 nm

The continuum removed reflectance spectra (CRR_λ) was characterized for magnitude of maximum band depth, location of band depth centre, area under the curve normalized to maximum band depth (ANMB) (Malenovský et. al., 2006) and asymmetry. The band depth (BD) at each wavelength in the absorption feature is calculated by subtracting the continuum removed reflectance (CRR) from '1' as was given by Kokaly and Clark (1999).

$$Band\ depth\ (BD_\lambda) = 1 - CRR_\lambda \quad \text{(3)}$$

$$Normalized\ band\ depth\ (NBD) = \frac{BD_\lambda}{BD_{max}} \quad \text{(4)}$$

$$Area\ under\ the\ curve\ normalized\ to\ maximum\ band\ depth\ (ANMB) = \int_{\lambda_{start}}^{\lambda_{end}} NBD \quad \text{(5)}$$

Where, 'BD_λ' is the band depth at a given wavelength, 'BD_{max}' is the band depth maxima and 'λ_{start}' and 'λ_{end}' are the wavelength of the start and end point in an absorption curve. Hereafter, the band depth maxima of blue and red region will be presented as $BD_{max\text{-}blue}$ and $BD_{max\text{-}red}$ respectively. Similarly, the area under the curve normalized to band depth at blue and red region will be represented as $ANMB_{blue}$ and $ANMB_{red}$ respectively. Conceptual diagram of the spectral absorption features in given in Figure 5.4.

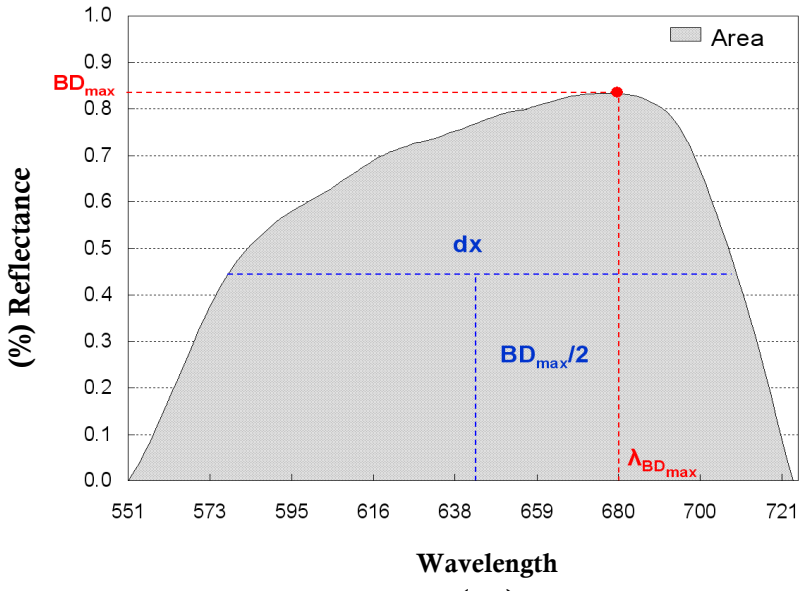

Figure 5.4: Absorption Parameters from Continuum Removed Spectra

(**BD_{max}** = maximum band depth, **λ_{BDmax}** = wavelength position of maximum band depth / absorption centre, **Area** = area below the absorption curve, **dx** = width at half height of the peak of the absorption curve, **Asymmetry** = ratio of area in the left side and right side of the BD_{max})

5.3.7 Hyperspectral Indices

5.3.7.1 Red-edge and Red-edge Position

Red-edge region is characterized by an abrupt change in canopy reflectance between the red (670 nm) and near infrared (740 nm) region, caused by combined effects of strong chlorophyll absorption in the red wavelengths and high leaf internal scattering in the near infrared region (Gates et al., 1965; Tucker, 1979; Horler et al., 1983). The shape and position of the red-edge are influenced by variations of chlorophyll content and leaf structure (Filella and Penuelas, 1994). The red-edge position (REP), defined by the point of maximum slope between the red chlorophyll absorption region, and the region of high near infrared reflectance (Horler et al., 1983), is a good indicator of foliar chlorophyll content and provides a very sensitive indicator of, among other things, vegetation stress. Red-edge is given as:

$$R_{re} = (R_{670} + R_{780}) / 2 \quad \text{..... (6)}$$

$$REP = 700 + 40 ((R_{re} - R_{700}) / (R_{740} - R_{700}) \quad \text{..... (7)}$$

Where, R = spectral reflectance, 700 and 40 are constants resulting from interpolation in the 700-740 nm interval.

5.3.7.2 Red-edge Normalized Difference Vegetation Index ($NDVI_{705}$)

The red-edge NDVI is designed for hyperspectral data with narrow sampling bandwidth which utilizes the bands along the red edge and sensitive to small changes in canopy. $NDVI_{705}$ is defined by an equation similar to the NDVI.

The value of this index ranges from -1 to 1. This was given by Gitelson and Marzlyak (1994). It was calculated as linear combination of spectral reflectance at 750nm and 705nm.

$$NDVI_{705} = (R_{750} - R_{705}) / (R_{750} + R_{705}) \quad \text{..... (8)}$$

5.3.7.3 Normalized Difference Water Index (NDWI)

Normalised Difference Water Index (NDWI) is sensitive to the canopy water content and is used for monitoring the changes in water content of the leaves. Short Wave Infrared reflectance represents the changes of water content while the changes of leaf and internal structure influence the near infrared reflectance (Gao et al. 1996). The combination of NIR and SWIR improves the accuracy to retrieve the crop water content (Wang et al., 2015). Since the reflectance in 860nm and 1240nm are only differs in the absorption of vegetation liquid water content, the scattering of 1240nm by the canopy may highlight the canopy water content (Gates, 1968). This index varies between -1 and 1. NDWI is given as follows:

$$NDWI = (R_{860} - R_{1240}) / (R_{860} + R_{1240}) \quad \text{..... (9)}$$

5.3.7.4 Normalized Difference Infrared Index (NDII)

NDII is also sensitive to the crop canopy water content and increases proportionally (Hardisky et al., 1983). The NDII values increase with increasing water content of crop canopy and vice versa. Basically, the NDII values gradually decreases due to water stress or disease incidence. It's values vary between -1 and 1. The formula of the index is given below:

$$NDII = (R_{819} - R_{1649}) / (R_{819} + R_{1649}) \quad (10)$$

5.3.7.5 Moisture Stress Index (MSI)

MSI is an index sensitive to the increase in the leaf water content by increase in the absorption in 1599 nm wavelength compare to 819 nm which is insensitive to the leaf water content and is used as a reference (Ceccato, 2001 and Hunt et al. 1989). Higher values of this index show higher water stresses and lower water contents as well as lower value of this index represents the lower stress and higher water contents. This index normally varies between 0 and 3. MSI is given as follows:

$$MSI = R_{1599} / R_{819} \quad (11)$$

5.3.7.6 Plant Stress Detection Index (PSDI)

Plant Stress Detection Index (PSDI) was introduced by Sanches et al. (2014) to analyze the different level of plant stress and to evaluate their usefulness to detect the plant stress intensity. PSDI is calculated using CR values near the feature centre around 680nm and on 560nm~575nm. Lower PSDI index values represent the higher plant stresses and higher PSDI index values represent the lower plant stresses. This index is not only to detect the stress level of plant but also identify the proper cause of the stress in canopy level which would be most valuable to detect the plant disease incidence and their severity. PSDI is calculated by using the following formula:

$$PSDI_{(i)} = (D_{(i)} - R_c^{'})/(D_{(i)} - R_c^{'}) \quad (12)$$

Where,

$R_c^{'}$=continuum removed reflectance at the feature centre; the feature depth (D) of each channel *i* in the absorption feature which is computed as follows,

$$D_{(i)} = 1 - CR \quad (13)$$

5.3.7.7 Disease Water Stress Index (DWSI)

Disease Water Stress Index (DWSI) has unique capabilities to discriminate the disease affected crop from the healthy one (Apan et al., 2004). According to the Apan et al. (2004), DWSI is

expressed as the ratio of reflectance of those spectral bands that are very sensitive to changes in leaf pigments, internal leaf structure and moisture content. DWSI-5 differentiates the disease affected crops from healthy one and categorise those affected crops based on the disease severity. The reflectance combination of green (550nm), red (680nm), NIR (800nm) and SWIR (1660nm) in DWSI-5 plays a major role to discriminate the severity of disease crop. Higher values of this index represent the higher severity of disease and lower value represents the opposite. DWSI-5 is given below:

$$DWSI\text{-}5 = (R_{800} - R_{550}) / (R_{1660} + R_{680}) \quad \text{..... (14)}$$

5.3.8 Field Measurement of Potato Late Blight Disease Severity

During the field visit visual assessment of potato late blight severity was estimated over the same footprint of hyperspectral sensor. The disease severity was grouped into nine classes (0-8) according to the disease rating scale described by James et al. (1947) where 0 = healthy/no lesions, 1 = up to 0.1% (few scattered plants blighted with 1 or 2 spots), 2 = 1% (seen up to 10 spots per plant or general light infection), 3 = 5%(up to 50 spots per plant, up 1 to10 leaflets infected), 4 = 25% (nearly every leaflet infected, but plants may smell of blight; field looks green although every plant is affected), 5 = 50% (every plant affected and about 50% of leaf area destroyed; field appears green, flecked with brown), 6 = 75% (about 75% of leaf area destroyed; field appears neither predominantly brown nor green), 7 = 95% (only a few leaves on plants, but stems are green) and 8 = 100% (all leaves dead, stems are dead or dying) affected. Disease severity index (DSI) at each footprint of hyperspectral observation was calculated by using the following formula:

$$DSI = I \times \overline{S} \times 100 \quad \text{..... (15)}$$

Where, I = disease incidence and $\bar{S}$= average disease severity. $\bar{S}$ was calculated by using the following formula:

$$\overline{S} = \frac{\sum_{i=1}^{n}(S \times n_i)}{n} \times 100 \quad \text{..... (16)}$$

Where, $\bar{S}$ = average disease severity, S = disease severity, n = total no. of diseased leaves and n_1, n_2, n_3, ..., n_8 were the number of diseased leaves with disease severity as 3%, 10%, 25%,.....,100%, respectively.

5.3.9 Predictive Ability

To compare the predictive ability of the disease severity index with measured disease severity index root mean square error (RMSE) was used which is defined as:

$$RMSE = \sqrt{(\sum(y_p - y_m)^2 / n} \quad \ldots\ldots(17)$$

Where y_p= predicted value

y_m = measured value

n = number of observation

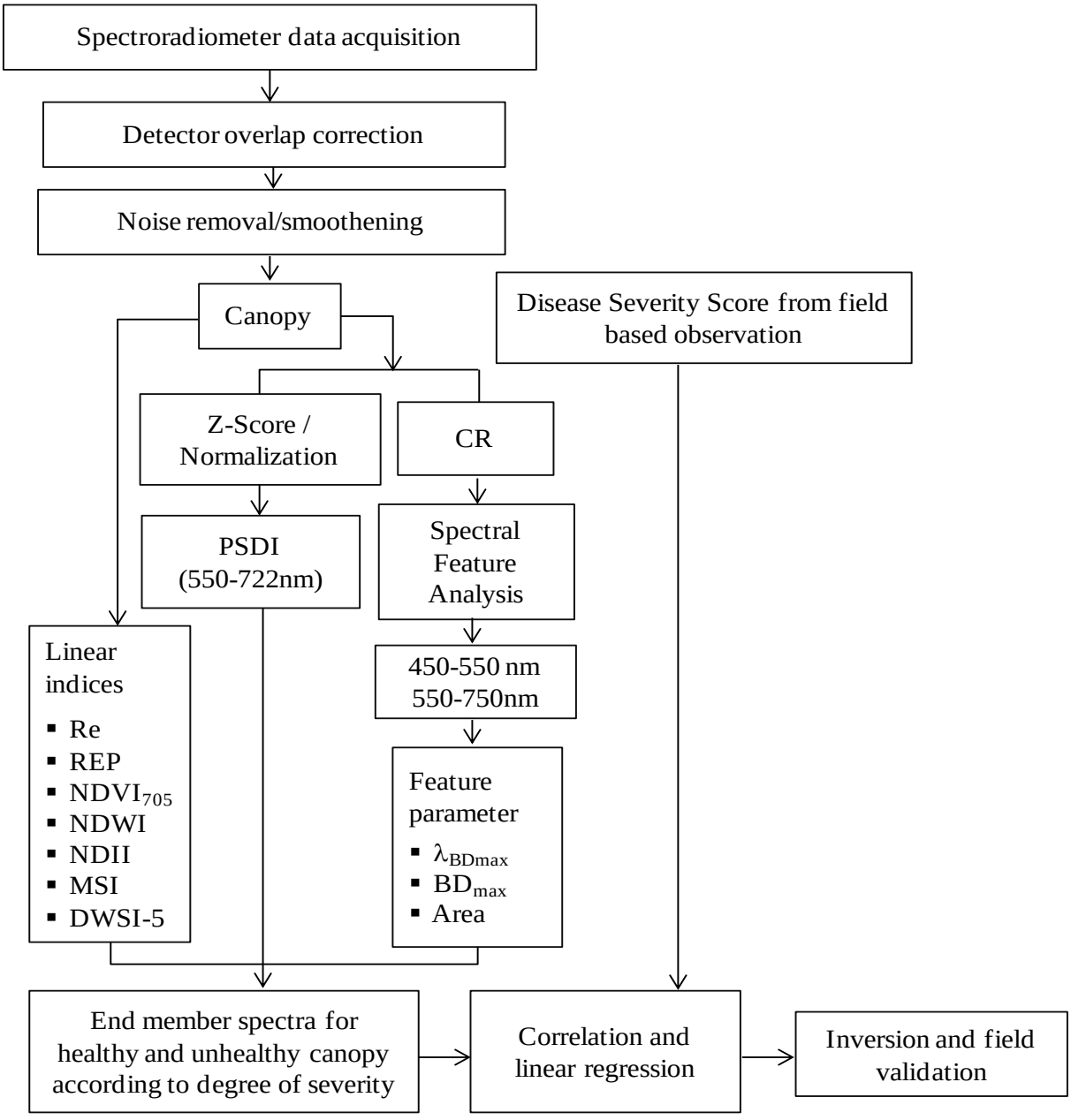

Figure 5.5: Overall Methodology for Hyperspectral Data Processing

5.4 Results and Discussion

5.4.1 Generation of Reference Spectra

Spectral profile of healthy green potato leaves and dry soil surface (fine tilth) were generated using average of 25 observations each (Figure 5.6). Noise minimization was done using following Savitzky and Golay (1964) technique and the spectra was normalized using primary statistics. The dry soil is characterized by monotonously increasing reflectance across 390-2500 nm with weak absorption minima at around 1450nm and 1950nm. The leaf reflectance of the potato shows sharp green reflectance peak at 550nm, followed by red absorption well due to plant pigment (670nm) and inflection at 720nm. For diseased affected potato plants, overall reflectance assumed a shape between health leaves and bare soil. However, the spectral difference between healthy and disease potato leaves is limited except at red absorption pit and IR reflectance maxima.

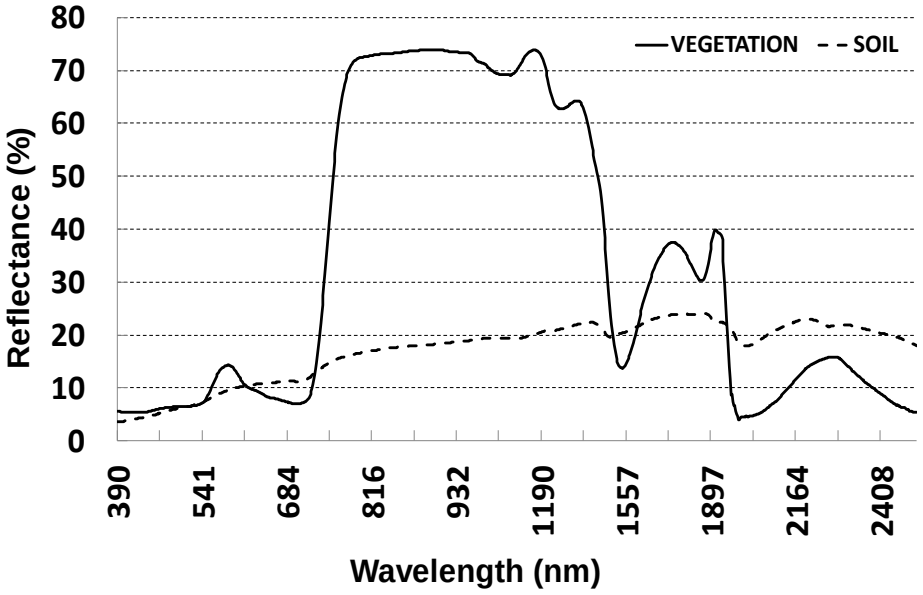

Figure 5.6: Spectra of Green Healthy Potato Leaves and Dry Soil

5.4.2 Spectral Profile of Disease Plants and Spectral Transformation

Spectral information of potato canopies, of various degrees of PLB severity, were collected from the field and grouped in relation to different levels of disease severity. The representative spectra of PLB affected potato crops are shown in figure 5.7 according to their severity. From the figure 5.7 it is observed that in comparison to healthy crops, the magnitude of reflectance is mostly lower except in the pigment and hydroxyl absorption bands.

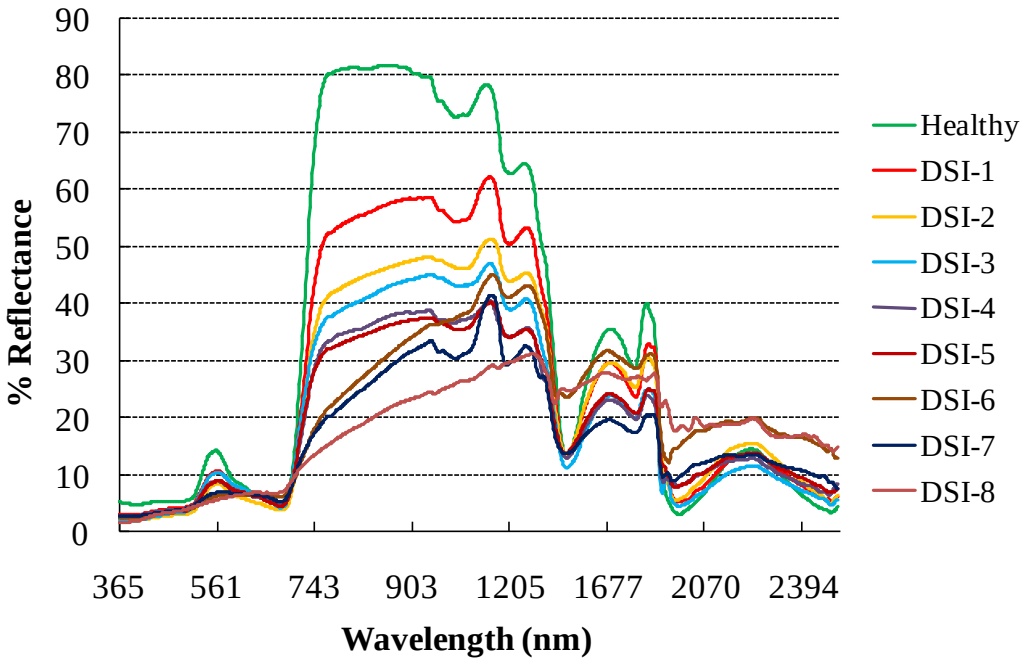

Figure 5.7: Spectra of Healthy Potato Crop and PLB Disease Affected Potato Crop According to Disease Severity Index

The first order derivative was chosen to process the original spectra to obtain in-depth band information in the respective wavelength range. This technique was done to remove the variability of spectra and to provide more sensitive measures of stress detection as well as its potential uses in estimating different disease severity levels. The first order derivative spectra of healthy and PLB affected potato crops are shown in figure 5.8. The derivative spectra shows the changing pattern of reflectance curve at different levels of PLB severity. The rate of change in reflectance curve is observed maximum in the DSI-8 (Disease Severity Index) in comparison to first order derivative spectra of healthy potato crops. In figure 5.8 maximum values in first order derivative is obtained in red-edge region where the rate of change is maximum, because of the abrupt increase in reflectance between red and NIR reflectance. In the present research first order maxima was observed between 720 and 730nm with highest value of 0.018 (at 723.4 nm) in healthy crops and lowest value of 0.0019 in most severely affected crop (DSI-8). In the green region, on the other hand, the maximum value (0.0033) of first order derivative was found at 521.7nm in healthy crops whereas the same for diseased crops is 0.0003 in severely affected (DSI-8) crops. In green region the lowest value was obtained at 560-580nm. These findings are in accordance with Peñuelas et al. (1994). In NIR region lowest value of -0.0079 was observed in healthy crop at 931.9nm whereas the lowest value (0.0003) was found in DSI-8.

From the first order spectral transformation it was apparent that the healthy crops exhibited highest value at both the red edge and green region when compare to disease affected crops (figure 5.8). First order derivative values in red edge region are useful indicator of chlorophyll content. With advancement of disease severity leaf chlorophyll content becames low, as a result, the maxima tend to lower values. The NIR region is sensitive to water content, as a consequence, the values of first order derivatives at 920 to 935nm region exhibited lower values in healthy crops due to the higher water absorption feature in comparison to diseased crops.

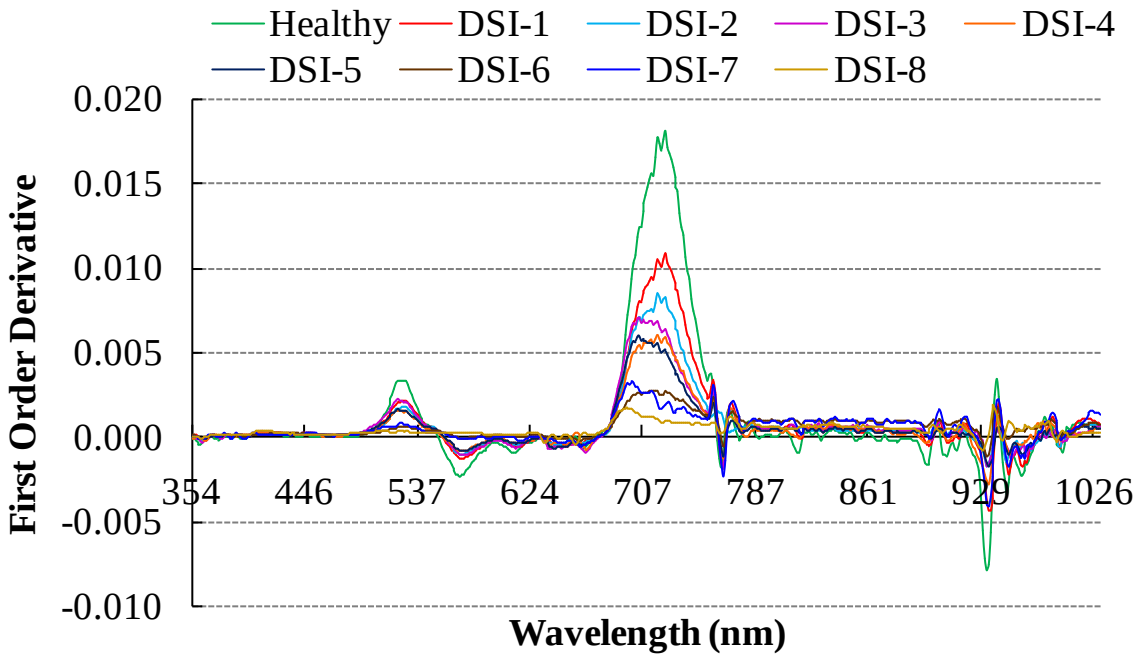

Figure 5.8: First Order Derivative Spectra in Different Levels of PLB Infestation

5.4.3 Spectra Discrimination of PLB Affected Potato Crops

The spectral profile of healthy and disease affected potato plants in different levels of severity were shown in figure 5.7 to discriminate the spectral characteristics of PLB affected potato crops. Spectral profile of some field observation along with their field photographs is presented in figure 5.9. The total reflectance region was partitioned into six regions; viz. 400–500nm, 520–590nm (green band in AWiFS), 620–680nm (red band in AWiFS), 700–740nm, 770–860nm (NIR band in AWiFS) and 920–1040nm. Quantitative differences of the average reflectance values of healthy potato plants and PLB affected potato plants in above mention regions were compared in table 5.1.

The spectral reflectance characteristics of healthy crops are significantly different when compared to diseased plants. In the visible region between 400 to 500nm and 520 to 590nm not much difference in spectral behaviour was noticed between healthy and diseased crops. The average values of reflectance in 400-500nm region are 0.053 and 0.031 for healthy and diseased (DSI-8) crops respectively. In the green region (520-590nm) the difference in spectral reflectance between healthy and diseased canopy is relatively high in comparison to blue region. The average reflectance values are 0.120 and 0.064 in healthy and diseased (DSI-8) canopy respectively. In the red region (620-680 nm), the spectral reflectance was higher in diseased plants over healthy one especially for DSI-6 and above. In red edge region between 700 and 740nm notable differences in healthy and diseased plants were observed. In respect of healthy one the reflectance of disease affected crops decreases 32.19% in DSI-1, 50.79% in DSI-4, 65.46% in DSI-6 and 70.17% in DSI-8 respectively. Significant difference in healthy and diseased crops was observed at two narrow ranges e.g 770-860nm and 920-1040nm. The spectral region of 770-860nm has potential to discriminate the PLB disease affected potato plants from the healthy ones. In this spectral region highest difference was recorded at 77.00% in DSI-8. The second spectral region located at 920–1040nm had the greatest discrimination properties between diseased and healthy plants. At this region the average values of reflectance of healthy crops is significantly higher (0.751) than diseased ones. The reflectance values progressively decreases with disease severity (0.562 in DSI-1, 0.440 in DSI-3, 0.365 in DSI-5 and 0.257 in DSI-8 respectively). The difference is highest at 65.71% in case of DSI-8.

Above observations indicate that spectral region of 770–860nm and 920–1040nm are most suitable to discriminate severity level of PLB affected potato crops.

Table 5.1: Average Values of Spectral Reflectance of Potato Canopy under Different Levels of Infestation

Wavelength region (nm)	Healthy Plants	PLB Affected Potato Plants							
		0.1%	1%	5%	25%	50%	75%	95%	100%
400–500	0.053	0.038	0.027	0.030	0.036	0.033	0.033	0.035	0.031
520–590	0.120	0.093	0.073	0.092	0.080	0.080	0.060	0.066	0.056
620–680	0.060	0.059	0.046	0.056	0.057	0.055	0.064	0.061	0.069
700–740	0.394	0.267	0.223	0.228	0.194	0.200	0.136	0.137	0.118
770–860	0.813	0.553	0.443	0.405	0.358	0.343	0.267	0.246	0.187
920–1040	0.751	0.562	0.472	0.440	0.375	0.365	0.377	0.320	0.257

Absolute Differences with respect to Healthy Plants								
400–500	0.014	0.026	0.023	0.017	0.020	0.020	0.018	0.021
520–590	0.027	0.047	0.028	0.040	0.040	0.060	0.054	0.064
620–680	0.001	0.014	0.004	0.003	0.005	-0.004	-0.001	-0.009
700–740	0.127	0.171	0.166	0.200	0.195	0.258	0.257	0.277
770–860	0.260	0.370	0.408	0.456	0.470	0.547	0.567	0.626
920–1040	0.189	0.279	0.311	0.376	0.386	0.374	0.431	0.493
Percentage Differences with respect to Healthy Plants								
400–500	27.37	48.96	43.93	31.65	38.42	37.11	34.25	40.43
520–590	22.49	38.95	23.50	33.25	33.36	49.99	45.16	53.58
620–680	1.07	23.65	6.02	5.16	7.94	-7.15	-1.82	-15.01
700–740	32.19	43.45	42.17	50.79	49.38	65.46	65.17	70.17
770–860	31.96	45.48	50.20	56.02	57.83	67.22	69.72	77.00
920–1040	25.11	37.16	41.43	50.04	51.39	49.75	57.36	65.71

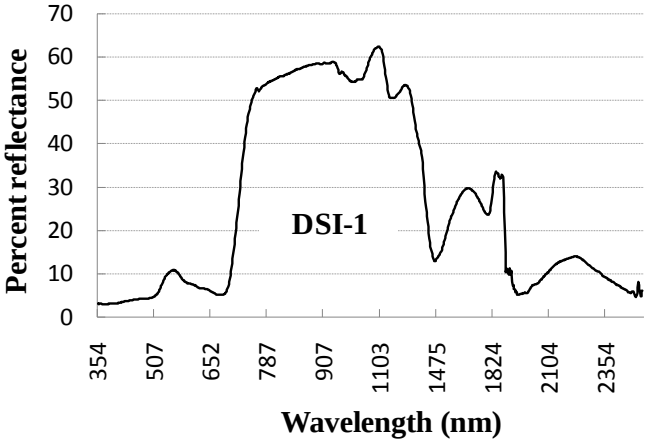

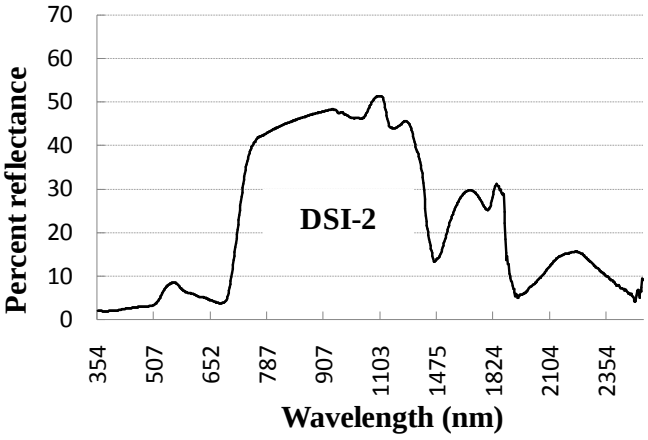


3

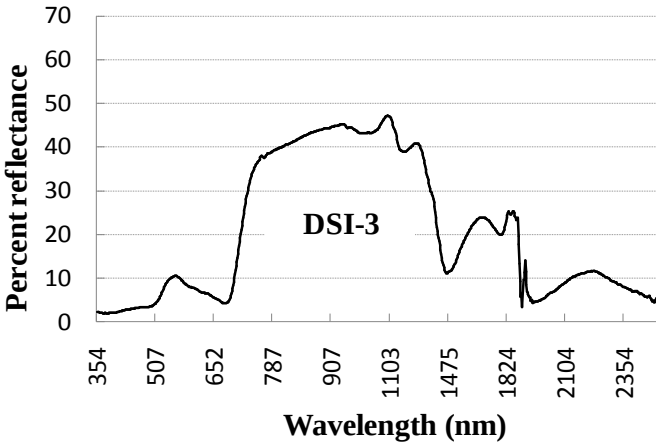
DSI-3
Percent reflectance
Wavelength (nm)
0
10
20
30
40
50
60
70
354
507
652
787
907
1103
1475
1824
2104
2354


4

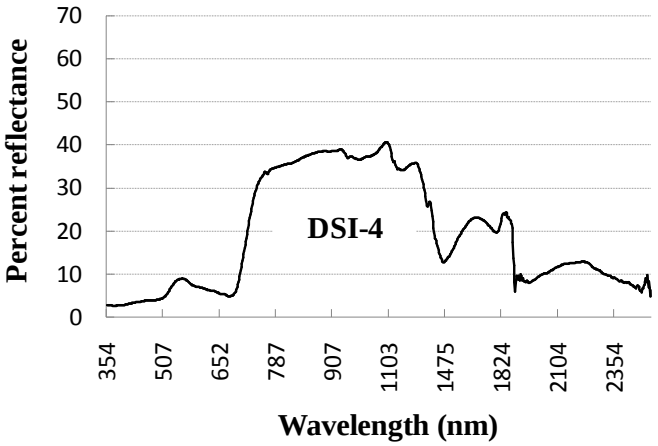
DSI-4
Percent reflectance
Wavelength (nm)
0
10
20
30
40
50
60
70
354
507
652
787
907
1103
1475
1824
2104
2354


5

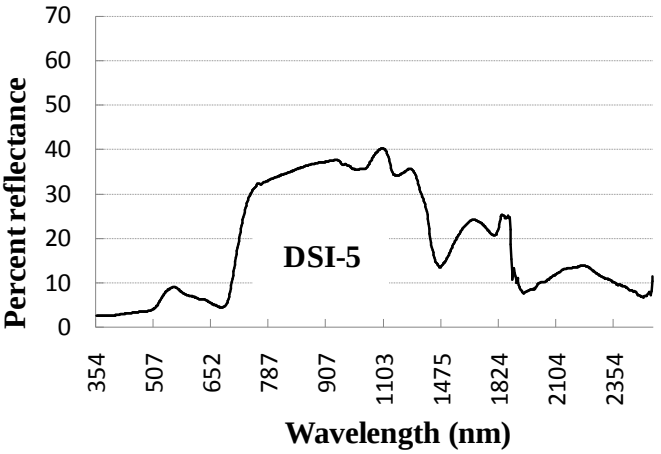
DSI-5
Percent reflectance
Wavelength (nm)
0
10
20
30
40
50
60
70
354
507
652
787
907
1103
1475
1824
2104
2354


6

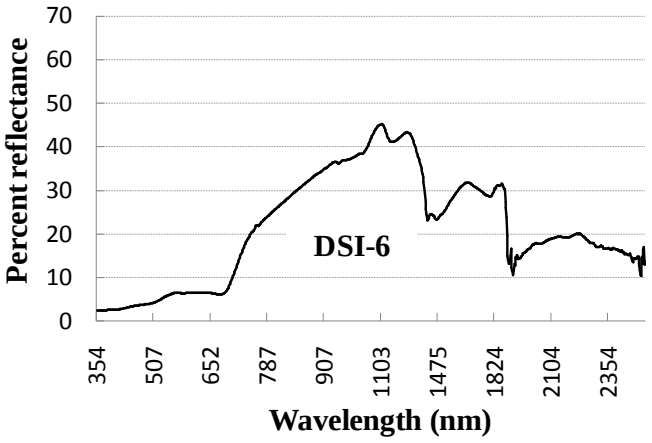
DSI-6
Percent reflectance
Wavelength (nm)
0
10
20
30
40
50
60
70
354
507
652
787
907
1103
1475
1824
2104
2354

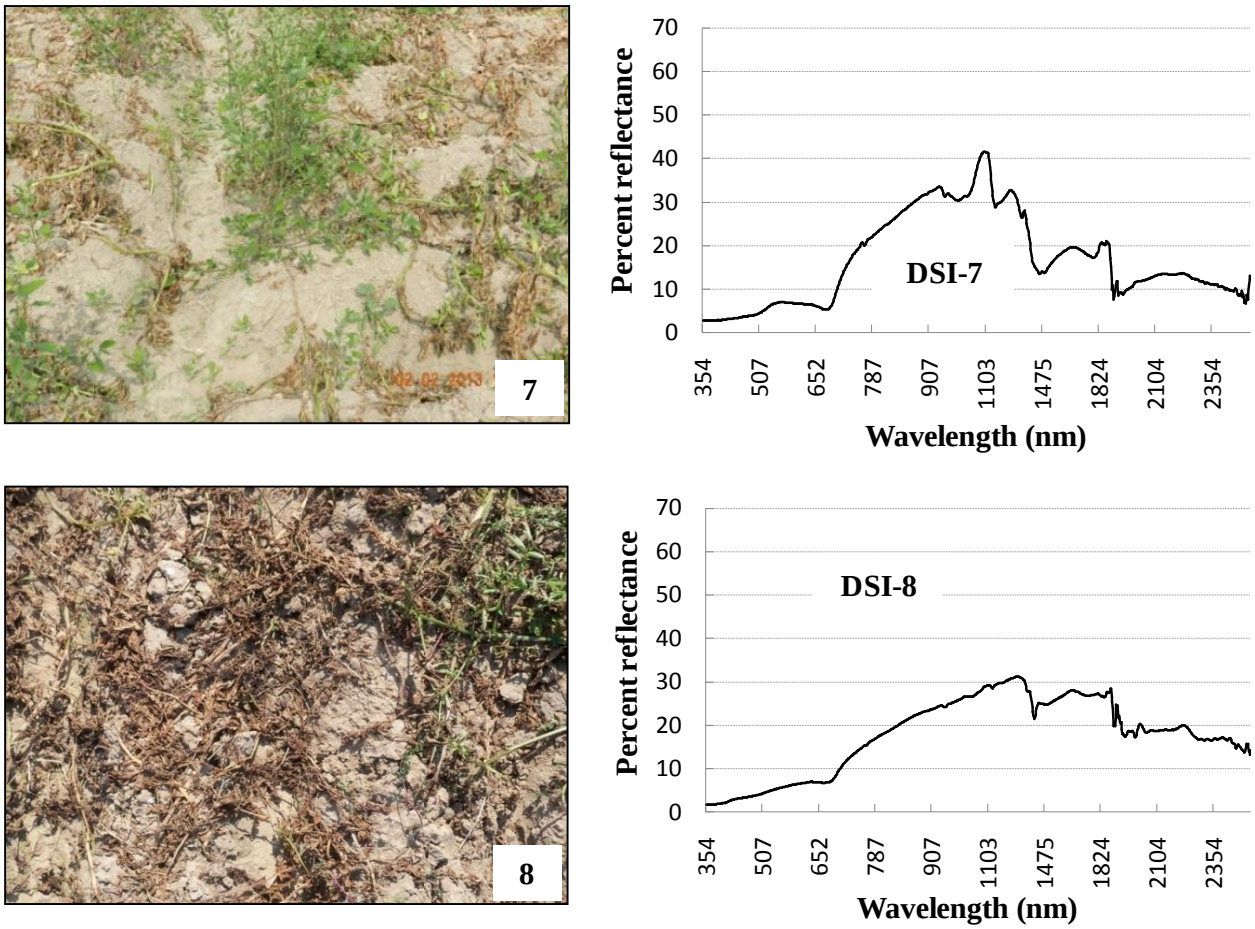

Figure 5.9: Spectral Response of Potato Canopy Affected by Different Severity of Potato Late Blight (PLB) Disease

5.4.4 Location Based Spectral Variables

In disease affected potato crops mean values of wavelengths at green reflectance peak (λ_{GP}) and red absorption well (λ_{RW}) are 557.7nm and 673.1nm respectively. The variability in wavelengths at which inflection point (λ_{IP}) occur varies from 696.8nm to as high as 722.7nm. The variation could be attributed to changes in plant pigment and leaf structural properties caused by the disease, assuming uniform agricultural management practices. The red edge parameters are considered to be good predictor variable for plant bio-physical descriptors as the spectral region of 670-780nm is sensitive to chlorophyll content and leaf internal structure (Castro and Sanchez-Azofeifa 2008). Table 5.2 shows values of red edge parameters and the location based spectral variables. There are significant differences between λ_{IP} and REP in terms of red edge position. REP is based on linear combination of reflectance values corresponding to 4 spectral bands centred around 670nm, 700nm, 740nm and 780 nm, whereas λ_{IP} is the location of maximum slope

between 670nm and 780nm based on first derivative of the reflectance spectra. It indicates that linear interpolation may not represent the true red-edge location.

5.4.5 Spectral Absorption Features

Three absorption feature parameters viz. wavelength of maximum band depth (λ_{BDmax}), band depth maxima (BD_{max}) and area under absorption curve for two pigment absorption regions were analyzed as a surrogate indicator of plant pigment. Table 5.2 describes large variation in wavelength of band depth centres (λ_{BDmax1}, λ_{BDmax2}) and absorption depth (BD_{max1}, BD_{max2}) of both the spectral regions. The area under blue absorption feature (450-550nm) is less than half in comparison the red absorption feature (550-750nm) which is very deep and broad. Similar to area the band depth is almost half in blue absorption feature.

Large variation in 'area under red absorption curve' is due to combined effect of pigment concentration and partial impact of leaf structure.

Table 5.2: Summery Table of Spectral Features

Spectral parameters	Minimum	Maximum	Average
Location based parameters			
λ_{GP}	552.6	565.1	557.7± 2.71
λ_{RW}	661.5	676.9	673.1± 2.84
λ_{IP}	696.8	722.7	709.6± 8.45
Slope at IP ($Slope_{IP}$)	0.09	1.35	0.59± 0.35
R_e	8.34	29.65	17.08± 5.63
REP	710.62	721.88	716.56± 2.66
Spectral absorption features (450-550 nm)			
λ_{BDmax1}	490.3	503.8	497.9± 2.12
BD_{max1}	0.08	0.56	0.34± 0.13
$Area_1$	32.3	37.17	35.09± 1.07
Spectral absorption features (550-750 nm)			
λ_{BDmax2}	671.3	686.5	677.7± 1.51
BD_{max2}	0.11	0.9	0.66± 0.21
$Area_2$	51.33	87.55	73.85± 8.49

5.4.6 Sensitivity of Spectral Variables to Potato Late Blight Disease

To decide the most sensitive spectral variables to PLB disease correlation values were calculated between spectral variables and DSI. The mean values of all the studied variables viz. red-edge (R_e), $NDVI_{705}$, NDWI, DWSI-5, NDII, MSI and PSDI along with their disease severity index is presented in Table 5.3. Along with linear indices two of the spectral variables viz. band depth maxima (BD_{max}) and area under the absorption curve ($Area_{red}$) in the red region (550-750nm) was also included to understand their response towards disease sensitivity. The mean values of all the spectral as a function of disease severity index were plotted in figure 5.10. The values of all the spectral indices were gradually decreased in respect of disease severity index, except MSI. The value of vegetation index ($NDVI_{705}$) in DSI-1 was 0.54 which gradually decreased to 0.30 in DSI-8 whereas in healthy crops it was found to be 0.61. In DWSI-5, the value in DSI-1 was 2.51 but it decreased up to 1.03 in DSI-8 whereas in healthy it was found to be 2.55. On the other hand, MSI was gradually increased with increasing of PLB disease severity level. In healthy crops mean observed value of MSI was 0.34, in contrast the values is 0.40 in DSI-1 which is due to decrease in leaf water content with advancement of PLB disease. In DSI-8 MSI value was very high (0.88).

Table 5.3: Mean Values of Spectral Parameters with respect to PLB Disease Severity Index

DSI	Red Edge	$NDVI_{705}$	NDWI	DWSI-5	NDII	MSI	PSDI	$BD_{max(red)}$	$Area_{(red)}$
0	43.01	0.61	0.125	2.55	0.45	0.34	0.66	0.86	85.27
1	31.74	0.54	0.093	2.21	0.37	0.4	0.65	0.83	84.89
2	24.41	0.5	0.067	1.96	0.32	0.47	0.61	0.8	82.65
3	22.74	0.48	0.048	1.8	0.28	0.52	0.57	0.76	82.17
4	20.7	0.46	0.046	1.75	0.28	0.52	0.56	0.73	80.83
5	18.9	0.44	0.017	1.7	0.25	0.57	0.51	0.71	80.34
6	16.77	0.43	0.015	1.61	0.23	0.58	0.36	0.69	79.62
7	14.26	0.37	-0.014	1.35	0.16	0.69	0.34	0.67	75.38
8	12.34	0.3	-0.018	1.03	0.09	0.88	0.17	0.62	71.32
$\mathbf{r^2}$	0.776	0.873	0.844	0.845	0.804	0.768	0.818	0.819	0.764

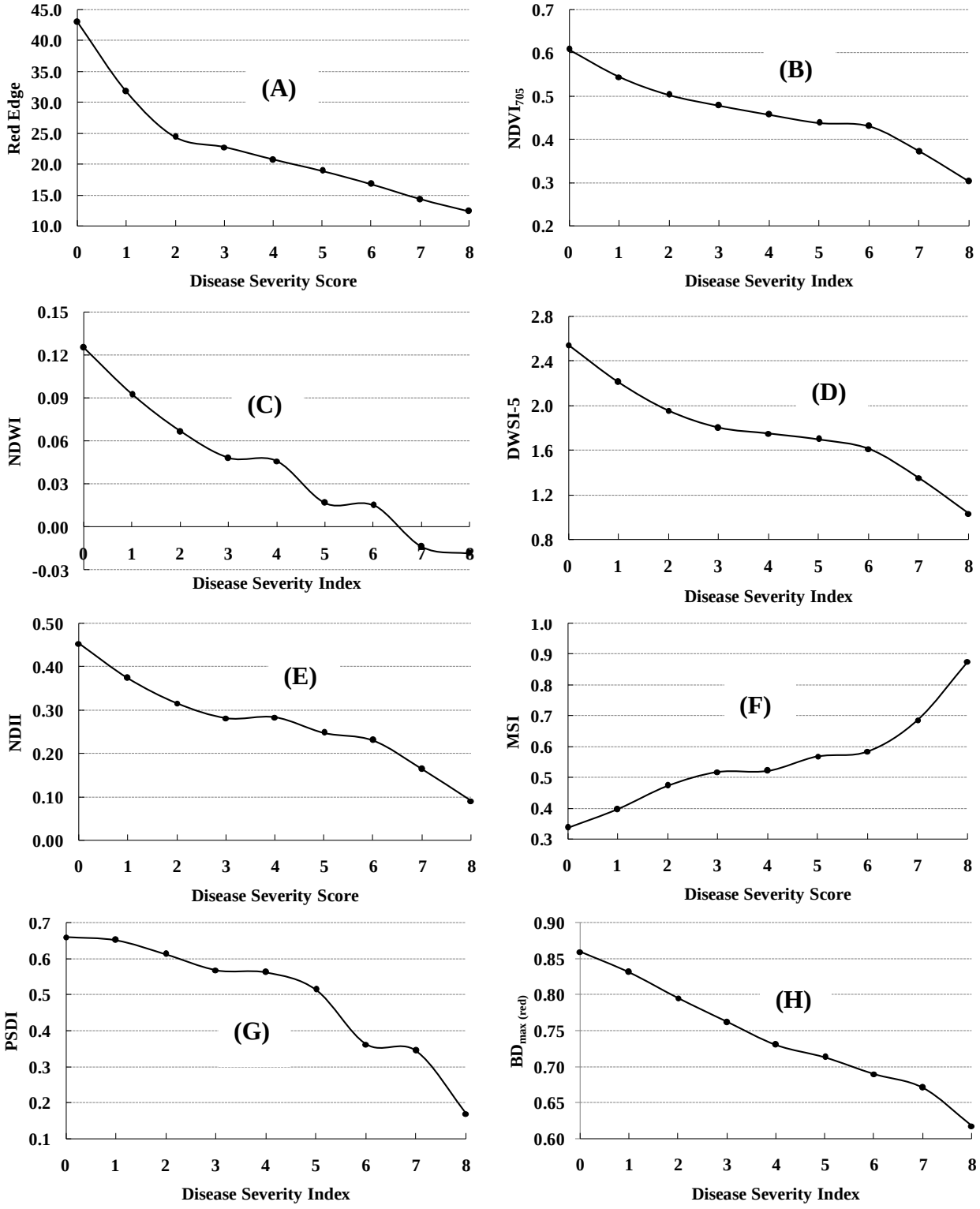
(A)
Red Edge
Disease Severity Score
(B)
NDVI705
Disease Severity Index
(C)
NDWI
Disease Severity Index
(D)
DWSI-5
Disease Severity Index
(E)
NDII
Disease Severity Score
(F)
MSI
Disease Severity Score
(G)
PSDI
Disease Severity Index
(H)
BDmax (red)
Disease Severity Index

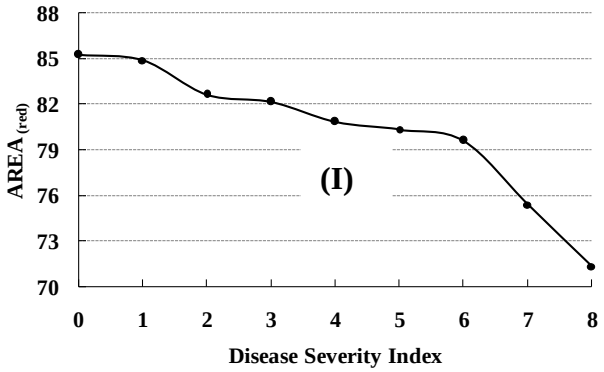

Figure 5.10: Line Graph Between DSI and A) Red Edge, B) $NDVI_{705}$,C) NDWI, D) DWSI-5, E) NDII, F) MSI, G) PSDI, H) $BD_{max(red)}$ at 550-750nm, I) $Area_{(red)}$ at 550-750nm

5.4.7 Relationship between Spectral Variables and Disease Severity Index

Correlation study was carried out (Table 5.4) among different spectral variables and disease severity indices. All the predictor variables show very high correlation (significant at 5% level) with disease severity index. Linear regression model was generated for each spectral parameter separately. The scatter plot between disease severity index and spectral variables are given in figure 5.12. All the spectral variables showed significant negative correlation with disease severity index except MSI which gives significant positive correlation. Band depth maxima at

Table 5.4: Correlation (r) Matrix among Spectral Parameters and Disease Severity Index

Vegetation Indices	DSI	Red Edge	$NDVI_{705}$	NDWI	DWSI-5	NDII	MSI	PSDI	$BD_{max\ (red)}$
Red Edge	-0.88								
$NDVI_{705}$	-0.93	0.86							
NDWI	-0.92	0.87	0.92						
DWSI-5	-0.92	0.84	0.95	0.90					
NDII	-0.90	0.85	0.92	0.89	0.94				
MSI	0.88	-0.81	-0.94	-0.85	-0.91	-0.95			
PSDI	-0.90	0.76	0.89	0.81	0.86	0.83	-0.87		
$BD_{max\ (red)}$	-0.91	0.84	0.93	0.86	0.85	0.83	-0.85	0.88	
$Area_{(red)}$	-0.87	0.75	0.92	0.80	0.87	0.85	-0.90	0.89	0.88

**all values are significant at 95% confidence level*

550-750nm showed very high correlation, which indicates that disease severity index is primarily sensitive to pigment concentrations. Out of all the spectral variables $NDVI_{705}$ does not show

saturation at lower disease severity index. However, $NDVI_{705}$ showed the highest negative correlation (r^2=0.87) which indicates that this index is most sensitive to PLB disease severity. DWSI-5 also showed the very high negative correlation (r^2=0.84) which indicates that this index is also equally capable to detect the severity level of PLB disease.

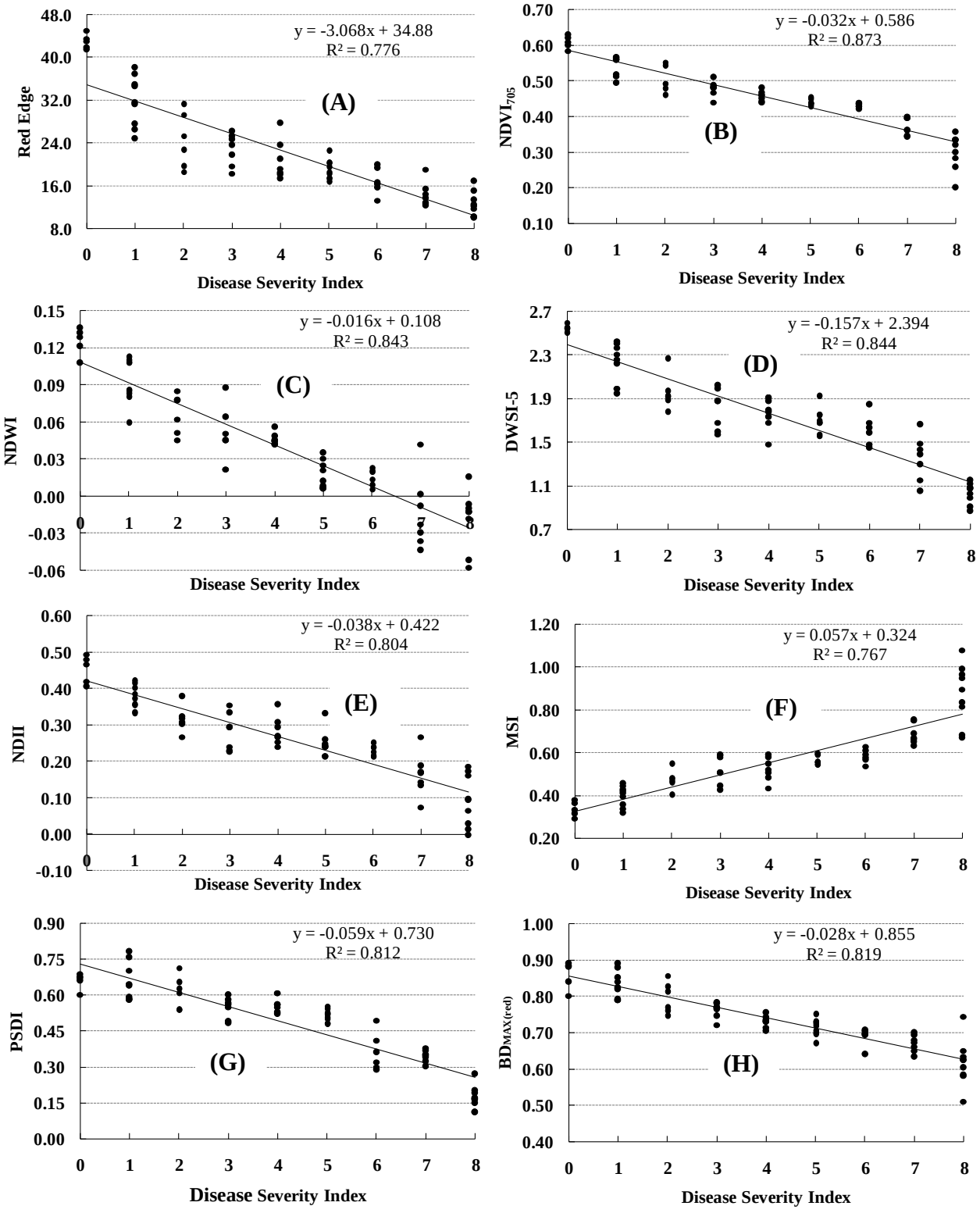

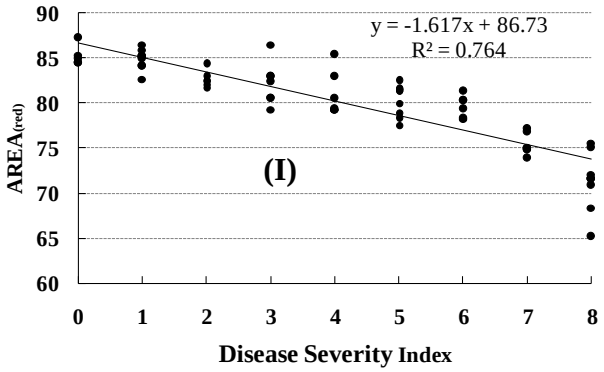

Figure 5.11: Relationship Between DSI and A) Red Edge, B) $NDVI_{705}$, C) NDWI, D) DWSI-5, E) NDII, F) MSI, G) PSDI, H) $BD_{max(red)}$ at 550-750nm, I) $Area_{(red)}$ at 550-750nm

5.4.8 Field Validation

Total 46 independent samples, having different disease severity index, were used for model validation, which were kept separate and not used for model development. Out of 9, three predictor variables viz. $NDVI_{705}$, DWSI-5 and NDWI were found to have significant contribution to predict the PLB disease severity index under different level of PLB infestation. A linear regression model was developed from the above mentioned spectral variables wherein the maximum variability is addressed by the red-edge NDVI ($NDVI_{705}$) and DWSI-5. The linear equation of model is given below:

$$DSI = 15.66 - (18.26 * NDVI_{705}) - (1.86 * DWSI\text{-}5) \quad (r^2 = 0.883) \ldots\ldots\ldots\ldots\ldots\ldots (18)$$

The prediction is so much high ($r^2 = 0.883$) when the combination of $NDVI_{705}$ and DWSI-5 is used for multi-linear regression model. $NDVI_{705}$ utilizes the bands along the red edge and sensitive to the changes of chlorophyll content as well as leaf structure. Moreover, NDVI detects these subtle variations of bio-optical responses caused by the diseased canopy. Similarly, DWSI-5 is also very sensitive to changes in leaf pigments, internal leaf structure and moisture content.

Mean RMSE was calculated using predicted and measured values of disease severity index. The value of RMSE in between measured and predicted disease severity is least i.e. 1.95.

5.5 Conclusion

Crop disease detection is a major activity to maintain food security and ecological environment protection in both agriculture and horticulture. Hyperspectral remote sensing technology has unique capabilities to detect and convenient rapid evaluation of physico-chemical response to crop disease. In this chapter, field spectroscopic study was performed to capture the minute details of healthy and disease infected potato canopy to compare the regions of spectral divergence. The advantages of using field instrumentation include the fact that spectrometry serves as a 'bridge' between lab measurements and the 'real world', and it facilitates refinement and testing of models associating biological attributes with remotely sensed data (Milton 1987). The purpose was to select the appropriate regions of the electromagnetic spectrum for PLB disease initiation and temporal severity. The difference in bio-optical response between healthy and diseased canopy is discernible at red and NIR region, the spectral reflectance of the diseased canopies were less than that of the healthy ones. In red edge region between 700 and 740nm notable differences in healthy and diseased plants were observed with highest of 70.17%. Significant difference in healthy and diseased crops was most prominent at two critical spectral regions e.g 770-860nm (77.00% in DSI-8) and 920-1040nm (65.71% in DSI-8) which is most suitable to discriminate the severity level of PLB affected potato crops. The first order derivative spectra of healthy and PLB affected potato crops showed the changing pattern of reflectance curve at different levels of PLB severity which can improve the separation between the disease severity levels. A relationship was found in between the first order derivative variation and the disease severity which summarized that the first order derivative of the reflectance spectra is more effective than the reflectance spectra in the early detection of late blight disease. Several location and area based spectral variables were identified sensitive either to plant pigment, bio-physical properties and both, to understand their effect on disease affected potato crops spectra. Out of all the spectral variables $NDVI_{705}$ and DWSI-5 showed very high negative correlation with PLB disease severity which indicates that these indices are very sensitive to PLB disease severity. To predict the PLB disease severity index under different level of PLB infestation a multi-linear regression model was developed from the above mentioned spectral variables and RMSE error in between predicted and measured values of disease severity index was found very less (1.95). This study established a scientific disease severity scoring methodology for remote monitoring of potato late blight disease using hyperspectral remote sensing technology. The major advantage of this approach is its simplicity and low computational load as well as its non-invasive remote procedure that makes it suitable for real-time potato late blight disease monitoring system.